Ab initio investigation of ammonia-borane complexes for hydrogen storage

Caetano R. Miranda and Gerbrand Ceder
Department of Materials Sciences and Engineering, Massachusetts Institute of Technology, Cambridge, Massachusetts 02139

(Received 13 December 2006; accepted 20 March 2007; published online 10 May 2007)

The structural, electronic, and thermodynamic properties of ammonia-borane complexes with varying amounts of hydrogen have been characterized by first principles calculations within density functional theory. The calculated structural parameters and thermodynamic functions (free energy, enthalpy and entropy) were found to be in good agreement with experimental and quantum chemistry data for the crystals, dimers, and molecules. The authors find that zero-point energies change several H_2 release reactions from endothermic to exothermic. Both the ammonia-borane polymeric and borazine-cyclotriborazane cycles show a strong exothermic decomposition character (approximately -10 kcal/mol), implying that rehydrogenation may be difficult to moderate H_2 pressures. Hydrogen bonding in these systems has been characterized and they find the N–H bond to be more covalent than the more ionic B–H bond. © *2007 American Institute of Physics*.
[DOI: 10.1063/1.2730785]

I. INTRODUCTION

Hydrogen storage, an important requirement for the commercialization of hydrogen-based energy, poses a challenge for materials science. The idea of storing hydrogen in a solid phase is attractive in order to meet the goals necessary for on-board storage for fuel cell operation in automobiles and electrical tools. Among the possible classes of materials, chemical hydrides stand out as a strong candidate.[1–3] In particular, ammonia-borane complexes have more recently been suggested as promising candidate materials for hydrogen storage[4–6] because of their high gravimetric (19.6 wt % H_2) and volumetric hydrogen densities and moderate decomposition temperature.[7–10] Recent experimental investigations on these systems show that by using a nanoscaffold of silica as catalyst,[4] or by milling and doping samples,[5,6] the kinetics of hydrogen release is improved and the exothermic nature of the hydrogen release reaction can be suppressed. However, hydrogen release reactions and the options for regeneration are not fully studied for these systems. These are crucial issues for the practical use of ammonia borane (BH_3NH_3) as a hydrogen storage system.

There have been several experimental studies on the thermal decomposition of ammonia borane (AB).[4–10] These studies agree on a two-stepwise exothermic decomposition. The first step releases about 1 mol of H_2 and the decomposition residue consists mainly of polymeric aminoborane $[BH_2NH_2]_x$ with some aminoborane (BH_2NH_2) and borazine ($B_3N_3H_6$) in the gas phase. In this paper, the ammonia-borane thermal decomposition reactions will be studied along two different paths: route A, the polymeric ammonia-borane cycle, and route B, the borazine-cyclotriborazane cycle. The release of hydrogen along these routes can be summarized as follows:

A. Route A—the polymeric ammonia-borane cycle

Reaction 1—The formation of Polyaminoborane (PAB):

$$x\ BH_3NH_{3(s)} \rightarrow [BH_2NH_2]_x + H_{2(g)}. \quad (1)$$

Reaction 2—The formation of Polyiminoborane (PIB):

$$[BH_2NH_2]_x \rightarrow [BHNH]_x + xH_{2(g)}, \quad (2)$$

which ultimately leads to the formation of boron nitride (reaction 3):

$$[BHNH]_x \rightarrow xBN + xH_{2(g)} \quad (3)$$

In practice, reaction 3 requires a large temperature ($\sim$1500 K) for hydrogen release. In addition, boron nitride (BN), the product of this reaction, is very stable and makes the reverse reaction impractical for hydrogen storage.

B. Route B—the cyclic polymeric ammonia-borane cycle

An alternative decomposition route of BH_3NH_3 is by formation of cyclic polymeric compounds, such as borazine ($B_3N_3H_6$), cyclotriborazane $(H_2BNH_2)_3$ (CTB), and polyborazylene ($[B_3N_3H_4]_x$) (PB). The hydrogen release reactions that form cyclic polymeric compounds are

Reaction 4—Dehydropolymerization of borazine:

$$3BH_3NH_{3(s)} \rightarrow B_3N_3H_{6(g)} + 6H_{2(g)}, \quad (4)$$

followed by

$$B_3N_3H_{6(g)} \rightarrow [B_3N_3H_4]_x + H_{2(g)}. \quad (5)$$

Reaction 5—Borazine-cyclotriborazane cycle:

$$B_3N_3H_{6(g)} + 3H_{2(g)} \leftrightarrow (H_2BNH_2)_{3(s)}. \quad (6)$$

Transformation of ammonia-borane into CTB:

$$3BH_3NH_{3(s)} \rightarrow (H_2BNH_2)_{3(s)} + 3H_{2(g)}. \quad (7)$$

Some theoretical efforts using quantum chemistry calculations have been made to characterize the thermodynamic properties of these compounds in the context of molecular systems.[11–15] Although molecular calculations can give important clues about the thermodynamics of these systems, most of these systems appear in the solid (crystalline or polymer) phase and an appropriate description of the AB compounds in these solid phases is needed since there is evidence of significant H–H bonding between hydrogens on different BH_3NH_3 molecules,[17] and the solid-solid reaction energies are likely to be different from those in the gas phase. Earlier density functional theory (DFT) calculations on the energetic and structural properties of ammonia borane,[15,16] did not apply zero-point energy corrections and predicted an endothermic reaction for the dehydrogenation of AB, in disagreement with experimental data.[7–10]

This work attempts to provide a more general evaluation of the energies of hydrogen release in ammonia-borane reactions including all decomposition products reported experimentally. The structures of the systems studied are shown and summarized in Fig. 1. Our first principles study intends to present not only the thermodynamic limits of the hydrogen realease reactions, but also a much-needed insightful atomistic picture of the energetics, structural, vibrational, and electronic properties in the hydrogenation and dehydrogenation processes in ammonia-borane compounds.

II. METHODOLOGY

We have explored the molecular and solid forms of ammonia-borane complexes by using DFT (Ref. 18) as implemented in the Vienna *Ab initio* simulation package (VASP).[19,20] Exchange and correlation were treated in the generalized gradient approximation (GGA) of Perdew-Wang 91 (Refs. 21 and 22) and projector-augmented potentials[23,24] with valence states $2s_22p_1$ for B, $2s_22p_3$ for N, and $1s$ for H were used. Convergence was tested for supercell size effects, Brillouin sampling, and energy cutoff. Plane waves with kinetic energy cutoff of 700 eV are used and the Brillouin-zone integration is done on a $4\times4\times4$ $(8\times1\times1)$ Monkhorst-pack k point mesh for the crystalline (polymeric) phases. The molecules (H_2 and borazine) were calculated in a large supercell $(12\times11\times13\ \text{Å}^3)$ to avoid interaction between the molecule and its image.

To determine and refine the structures of ammonia-borane complexes, full ionic relaxation was performed by using the conjugate gradient method until the forces were converged to 0.025 eV/Å. For crystalline structures, a volume relaxation has been also carried out in addition to the ionic relaxation. Experimental input on these systems or analogous molecules was used as starting positions for the relaxations. The AB solid was relaxed from the position given by the neutron crystallographic data.[25] For PAB, the analog structures for polyethylene (both orthorhombic and monoclinic) and AB have been used. The polymeric PAB and PIB chains were optimized starting from the relaxed molecules organized in different oligomers and including their possible conformations.[26–28] For the cyclic compounds such as borazine, CTB, and PB, the initial structures were taken from available experimental data and quantum chemistry calculations.[29–31]

Phonon frequencies of ammonia-borane complexes were obtained with the direct method[32] on $3\times3\times3$ supercells for crystalline structures and $6\times1\times1$ cells for polymeric systems. The Hellmann-Feymann forces on all atoms in the supercell were calculated with displacements of 0.04 Å for each ion in three independent directions. Tests with smaller displacement were performed and no significant change of the force constants was observed indicating that the displacements were in the harmonic regime. Based on these forces, the dynamical matrix for each system was evaluated only at the Γ point of the Brillouin zone and the phonon frequencies and their modes were obtained by diagonalizing it.

III. RESULTS

A. Geometry and chemical bonding

To discuss the structural properties of ammonia-borane complexes we compare our results obtained with DFT in Tables I and II with the available experimental information. For all the systems studied the calculated geometrical properties are in good agreement with the experimental data and with other theoretical results obtained by quantum chemistry calculations.[11–17,25,31] In particular, our results agree very well with the results obtained by the most refined quantum chemistry methods.[11] This is an indication that the chemistry is correctly described by the DFT-GGA approximation. Our data for the crystalline structures in Table II also agree well with the experimental data available[25] and DFT calculations on ammonia borane using the same functional.[17]

Note that the BN dative bond, formed by the donor-acceptor complex between the lone pair of NH_3 and the $2p$ empty orbital of BH_3, is shorter in the AB crystal than in the molecule. The opposite effect occurs for the PAB and PIB, for which the B–N bond gets longer going from the molecule to the polymer. The former effect has been proposed to be due to the short-range dipole-dipole interactions in the molecular ammonia-borane crystal.[33] Interestingly, the DFT-GGA calculations are able to correctly capture this feature.

An important issue to address is the nature of the bonds between B, N, and H. The bond character can be obtained by analyzing the electron localization function (ELF).[34–37] This function is defined between 0 and 1, where a value of 1 means strong localization characteristic of covalent bonds or lone electron pairs. Values close to 0.5 reflect an electron-gas type. The ELF plots are similar for the different AB systems and we discuss two of them in more detail: PIB and PB, as they capture the different electronic environments and chemical bonding observed in our calculations for AB complexes (Fig. 2). The calculated electronic structure data of the ammonia-borane complexes are available as supplementary material.

The first interesting point is the symmetry difference in the ELF for the hydrogen atoms bonded with boron and nitrogen. In the case of nitrogen, the calculated ELF is more spherically symmetric, centered on the H sites, while for boron the ELF is elliptical and polarized away from the H site.

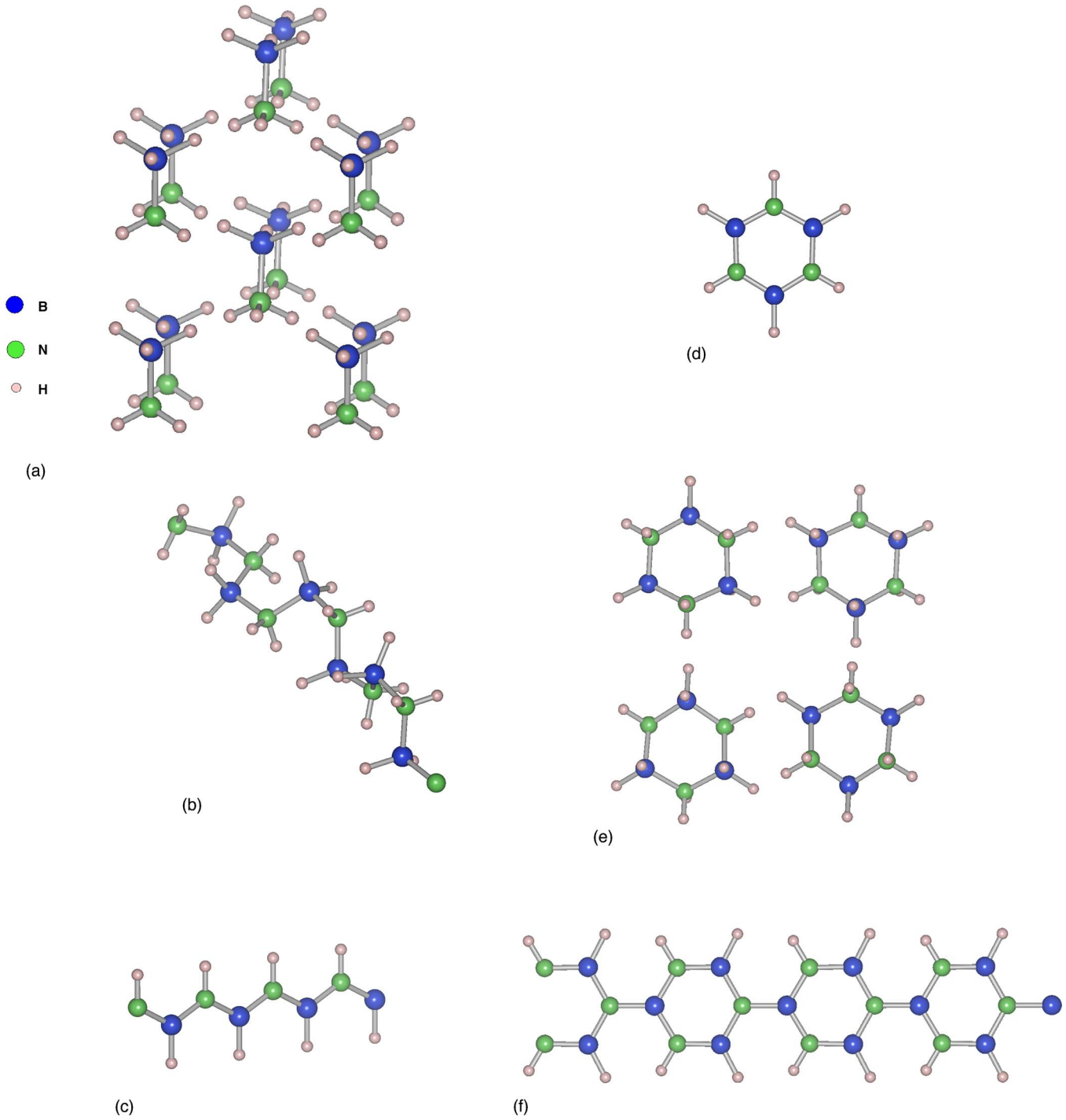

FIG. 1. (Color online) Structures of ammonia-borane complexes: (a) ammonia borane, (b) polyaminoborane, (c) polyiminoborane, (d) borazine molecule, (e) cyclotriborazane, and (f) *p*-polyborazylene. The blue atoms are B, the green atoms are N, and rose are the H atoms.

The polarization away from the boron indicates a more ionic bond than for the hydrogen bonded to N. The observations on the ELF plot are consistent with the projected density of state for the hydrogen bonded to nitrogen and boron, respectively (Fig. 3). Hydrogen bonded with boron accounts for most of the states in the region close to the Fermi level. The states of the hydrogen bonded to the nitrogen are in regions of lower energy and closer to where the states of nitrogen are localized. Of interest is the nature of the B–N bonds in PIB and PB. In the ELF for both systems the covalent character of the B–N bonds is clearly shown by the high values in the region between the BN sites. The ELF characteristics for hydrogen are found to have the same behavior regardless of the kind of compound (chain or cyclic). This reflects a local nature of the bonding between H and these atomic species.

B. Vibrational and thermodynamics properties

Figure 4 displays the vibrational density of states obtained by the direct method for ammonia-borane complexes. The experimentally measured infrared peaks are indicated by arrows for comparison. In this section, we will discuss the

TABLE I. Calculated and experimental geometric parameters of ammonia-borane complexes: bond lengths r (Å) and bond angles θ (deg).

System	r_{BN}	r_{BH}	r_{NH}	θ_{H-B-H}	θ_{H-N-H}	$r_{HH'}$	θ_{B-N-B}
$BH_3NH_{3(s)}$	1.5978	1.2220	1.0291	110.64	107.22	2.2012	⋯
Expt.	1.58(2)	1.18(03)	1.07(04)			2.23(04)	
$BH_3NH_{3(dimer)}$	1.6328	1.2315	1.0392	111.96	107.95	1.8769	
$BH_3NH_{3(g)}$	1.6461	1.2161	1.0237	113.34	107.83	⋯	⋯
Expt.	1.6576	1.2160	1.0140	⋯	⋯	⋯	⋯
$[BH_2NH_2]_x$	1.6035	1.2059	1.0248	115.02	106.52		110.12
$BH_2NH_{2(g)}$	1.3928	1.2000	1.0141	122.32	113.33	⋯	⋯
Expt.	1.403						
$[BHNH]_x$	1.4317	1.1964	1.0201	⋯	⋯	⋯	⋯
$HBNH_{(g)}$	1.2464	1.1730	0.9987	⋯	⋯	⋯	⋯
Expt.	1.2381						
Borazine	1.4342	1.1993	1.0139				123.15
CTB	1.5844	1.2208	1.0397	111.45	104.30		115.59
Expt.	1.570	1.12					
Polyborazylene	1.4073	1.2010	1.0137				121.12

general characteristics of the vibrational density of states focusing on the differences between the systems studied.

We observe an overall agreement with the experimental results for all the systems involved (AB, PAB, PIB, CTB, and PB).[8,10,33,38] It is important to clarify that the experimental data for PB is in solution of HCl,[38] which makes the direct comparison not so straightforward. The higher frequency regime ($\sim$3500–3700 cm^{-1}) is associated with the stretching of N–H bonds. These modes shift to higher frequencies from CTB to AB, PAB, and PIB. This effect is due to the shortening of the NH distance, as can be observed in Table I. A similar trend is observed in the region of 2500 cm^{-1}, which corresponds to the stretching of the B–H bond. Around 1610 and 1000 cm^{-1}, there are modes related to the NH_3 (NH_2) bend. Note that these modes disappear in the PIB case. The same happens for the modes around 1100 cm^{-1} which are related to the $BH_3(BH_2)$ bending mode. The stretching mode for the BN double bond is found to be in the region of 1350 cm^{-1}. The discrepancy with the experimental values at high frequencies is related to the overestimation of the BH and NH bond lengths in our first principles calculation as compared to experiment, at least for the case of ammonia borane. The modes related to the BN bond are well described within DFT, as can be expected from the good agreement between calculated and experimental B–N bond lengths.

The bond frequencies make it possible to assess the vibrational contribution to the thermodynamic properties as a function of temperature within the harmonic approximation. We will treat the cases of solids and molecules separately. The total Gibbs free energy is given by

$$G(N,V,T) = H(N,V,T) - T\,.\,S(N,V,T). \tag{8}$$

For the solids, the enthalpy H can be written as a combination of several terms,

$$H(N,V,T) = E^0_{elec} + E_{vib}(T) + pV, \tag{9}$$

where E^0_{elec} is the ground state energy obtained by first principles calculations, p the pressure, and V the volume. Since the effect of pressure on the free energy of solids is small we neglect the pV term. The term $E_{vib}(T)$ is the vibrational enthalpy contribution above the ground state energy, as obtained within the harmonic approximation by:[28]

TABLE II. Optimized structural information obtained in this study by first principles calculations.

System	a (Å)	b (Å)	c (Å)	α (deg)	β (deg)	γ (deg)	Volume (Å^3)
BH_3NH_3(crystal)	5.302	4.939	5.172	90.0	90.0	90.0	135.44
BH_3NH_3(expt)	5.395(2)	4.887(2)	4.986(2)	90.0	90.0	90.0	131.5(16)
$BH_2NH_{2(polymer)}$	2.629	⋯	⋯	⋯	⋯	⋯	⋯
$HBNH_{(polymer)}$	2.518	⋯	⋯	⋯	⋯	⋯	⋯
Cyclotriborazane	4.402	12.230	11.211	90.0	90.0	90.0	603.57
Polyborazylene	4.300	⋯	⋯	⋯	⋯	⋯	⋯

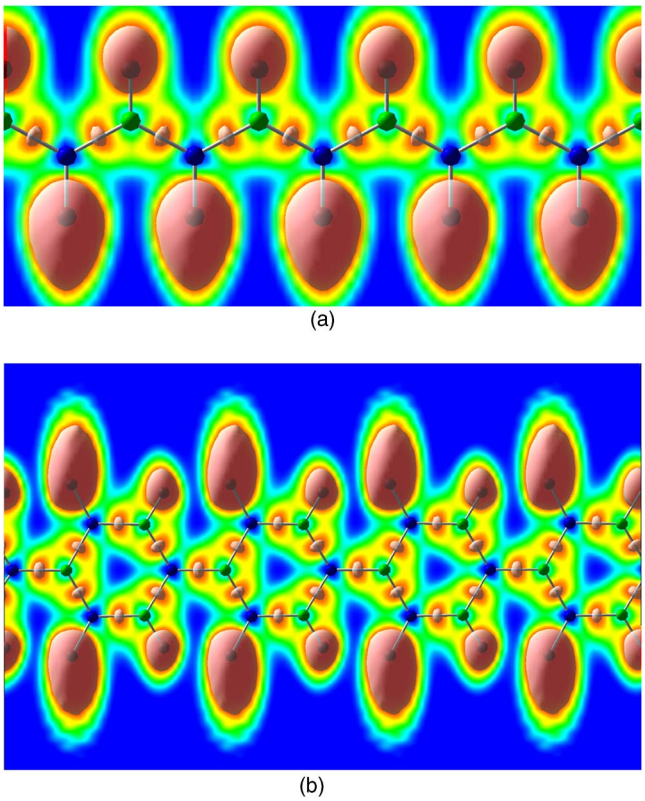

FIG. 2. (Color online) Examples of electronic environment in the ammonia-borane complexes: electron localization function (ELF) of (a) polyiminoborane (PIB) and (b) polyborazylene (PB). The isosurface of ELF=0.9 is shown. Rainbow scale used: ELF=1(red) to ELF=0(blue).

$$E_{\mathrm{vib}}(T) = \frac{1}{2} r \int_0^\infty \hbar \omega g(\omega) \coth\left(\frac{\hbar \omega}{2 k_B T}\right) d\omega, \tag{10}$$

where T is the temperature, r is the number of degrees of freedom, $\hbar$ is the Planck constant, k_B is the Boltzmann constant, and $g(\omega)$ and ω are, respectively, the phonon density of states and the frequencies obtained by the direct method.

The finite temperature-dependent term can be separated from the zero-point energy (E_{ZPE}) by taking the limit of Eq. (10) as the temperature goes to zero.

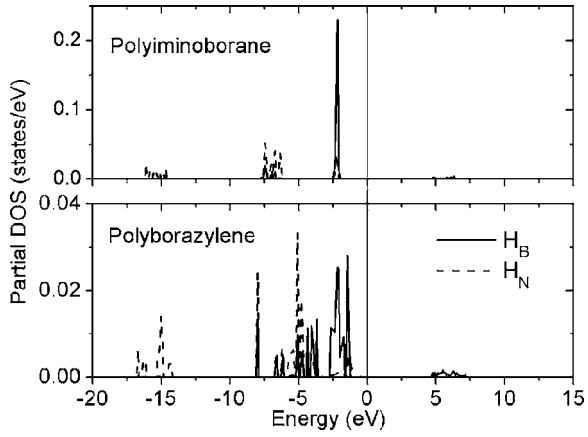

FIG. 3. Projected electronic density of states for the hydrogen bonded with nitrogen (H_N) and boron (H_B) for polyiminoborane and polyborazylene.

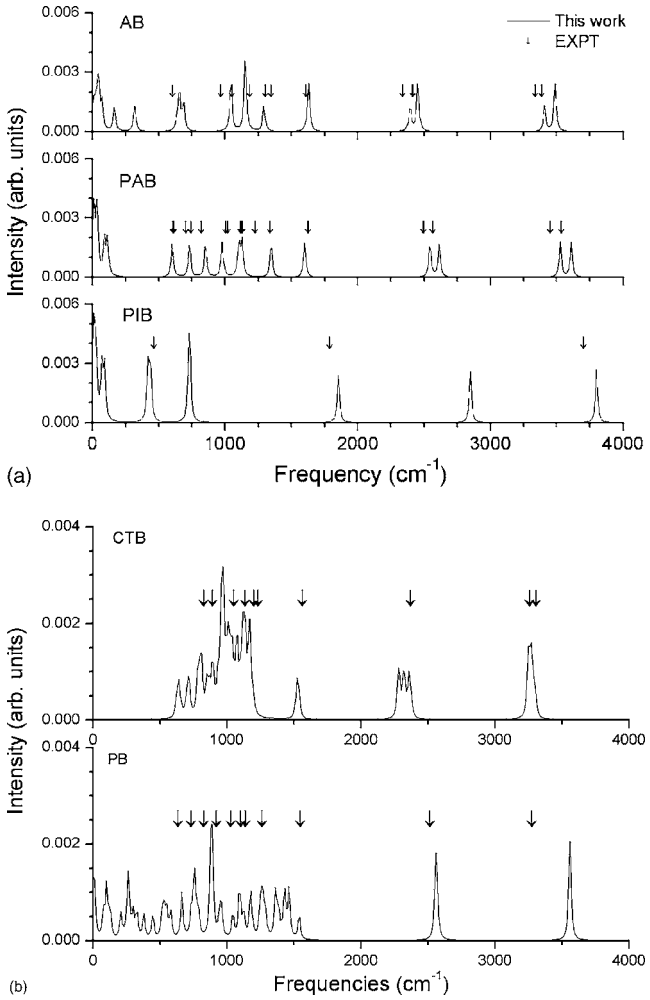

FIG. 4. Calculated vibrational density of states for ammonia borane (AB), polyaminoborane (PAB), polyiminoborane (PIB), cyclotriborazane (CTB), and polyborazylene (PB). The infrared experimental data available is indicated by arrows. For PB, the experimental value is for $B_3N_3H_{6.3}HCl$ (see text).

$$E_{\mathrm{ZPE}} = \lim_{T \to 0} E_{\mathrm{vib}}(T) = \frac{1}{2} r \int_0^\infty \hbar \omega g(\omega) d\omega. \tag{11}$$

.

For the molecules (hydrogen and borazine), additional terms based on ideal-gas behavior have been included to describe the translational [$(3/2)k_BT$], rotational [k_BT for H_2 and $(3/2)k_BT$ for borazine], and the pV terms (k_BT). In the gas phase the term relative to the enthalpy is then given by

$$H_{\mathrm{mol}}(N,V,T) = E^0_{\mathrm{elec}} + E_{\mathrm{vib}}(T) + E_{\mathrm{molecule}}(T). \tag{12}$$

The E_{molecule} is the contribution from the molecular degrees of freedom and is given by $(7/2)k_BT$ for H_2 and $4k_BT$ for borazine.

In the harmonic approximation, the vibrational entropy as a function of the temperature is.[32]

TABLE III. Polymeric and cyclic ammonia-borane complex route reaction energies in kcal/mol for the crystalline systems.

Reaction No.	Reactants		Products		ΔH This work
1	$H_3BNH_{3(s)}$	→	$[H_2BNH_2]_x$	$H_{2(g)}$	
E_{elec}	−871.88		−711.35	−156.76	+3.77
$+E_{ZPE}$	−824.76		−675.62	−150.71	−1.57
2	$[H_2BNH_2]_x$	→	$[HBNH]_x$	$H_{2(g)}$	
E_{elec}	−711.35		−553.09	−156.76	+1.50
$+E_{ZPE}$	−675.62		−534.48	−150.71	−9.57
4	$B_3N_3H_{6(g)}$	→	$2[B_3N_3H_4]_x$	$H_{2(g)}$	
E_{elec}	−1662.64		−1509.36	−156.76	+3.48
$+E_{ZPE}$	−1604.27		−1462.90	−150.71	−9.34
5	$B_3N_3H_{6(g)}$	$3H_{2(g)}$	→	$B_3N_3H_{12(s)}$	
E_{elec}	−1662.64	−470.28		−2147.23	+14.31
$+E_{ZPE}$	−1604.27	−452.13		−2039.42	+16.98
6	$3H_3BNH_{3(s)}$	→	$B_3N_3H_{12(s)}$	$3H_{2(g)}$	
E_{elec}	−2615.64		−2147.23	−470.28	−1.87
$+E_{ZPE}$	−2474.28		−2039.42	−452.13	−17.27

$$S(T) = rk_B \int_0^\infty g(\omega) \left\{ \left(\frac{\hbar\omega}{2k_BT} \right) \left[\coth\left(\frac{\hbar\omega}{2k_BT} \right) - 1 \right] - \ln\left[1 - \exp\left(\frac{-\hbar\omega}{k_BT} \right) \right] \right\} d\omega. \quad (13)$$

.

Tables III and IV summarize the total electronic enthalpy, the corresponding zero-point correction, and the reaction enthalpy at 0 K for the crystalline and gas phases for the polymeric ammonia-borane complexes cycle (route A). The quantum chemistry results for the gas phase are also included for comparison. The DFT results are in good agreement with quantum chemistry calculations.[11–15]

The results in Table IV indicate that the zero-point energy corrections are an important factor to be considered. In particular, this contribution is responsible to get the correct exothermic character of polyaminoborane formation (reaction 1) for both the crystalline and molecular case. In addition, Table IV also shows the importance of calculating the energies in the solid phase of the products. If only reactions between molecular species are considered,[11] the iminoborane formation (reaction 2) has a strong endothermic character (30.25 kcal/mol at 300 K) in disagreement with thermal decomposition experiments.[4–10]

The thermodynamic properties (Helmholtz free energy, enthalpy, and entropy) of the crystalline phase of AB are shown in Fig. 5 with the corresponding quantities at 0 K as a reference. The calculated results compare well with the available experimental data (squares). This indicates that the harmonic approximation provides a good description of the thermodynamics of ammonia borane. A deviation of the experimental values is expected for temperatures above 230 K, where a structural transition from the orthorhombic to tetragonal structure takes place for the crystalline AB.[39]

We show in Fig. 6 the thermodynamic properties for the other crystalline and polymeric phases of the ammonia-borane complexes. To the best of our knowledge, experimental data for these quantities are not available in the literature. However, based on the good agreement with experiments for ammonia borane, and the correct description of the vibrational properties for these systems, we expect that our calcu-

TABLE IV. Polymeric ammonia-borane complex cycle reaction energies in kcal/mol for the molecular systems.

Reaction No.	Reactants		Products		ΔH This work	ΔH Quantum chemistry[a]
1	$H_3BNH_{3(g)}$	→	$H_2BNH_{2(g)}$	$H_{2(g)}$		
E_{elec}	−855.27		−696.68	−156.76	+1.83	
$+E_{ZPE}$	−811.77		−666.79	−150.71	−5.73	−6.8
2	$H_2BNH_{2(g)}$	→	$HBNH_{2(g)}$	$H_{2(g)}$		
E_{elec}	−696.68		−500.83	−156.76	+39.09	
$+E_{ZPE}$	−666.79		−485.09	−150.71	+30.99	29.5

[a]Reference 11.

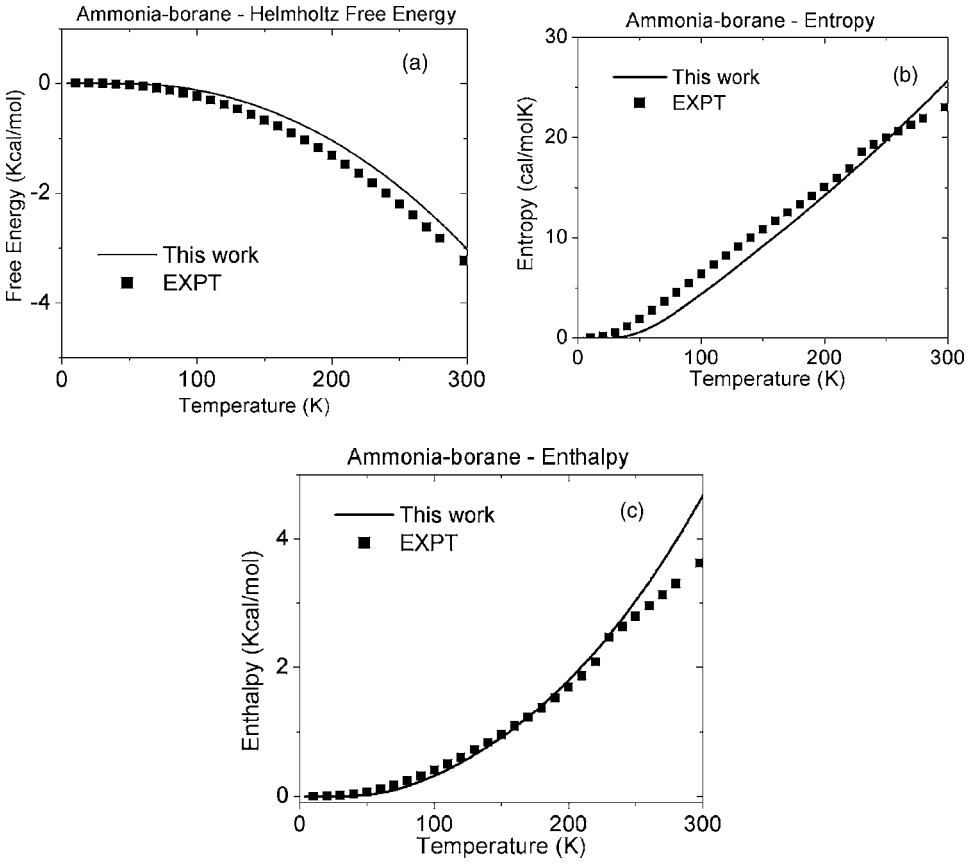

FIG. 5. Calculated free energy (a), enthalpy (b), and entropy (c) of ammonia-borane complexes as a function of temperature compared with experimental results (Ref. 10). The energies at 0 K are set to zero.

lations provide a suitable description of the thermodynamic data for the systems studied: PAB, PIB, CTB, and PB.

C. Decomposition reactions

Supported by the calculated thermodynamic properties, we can determine the changes in enthalpy and free energy for the thermal decomposition reactions of ammonia-borane complexes. In this section, we discuss the reactions presented in Eqs. (1), (2), and (5)–(7). In Fig. 7, the differences between the products (b) and reactants (a) are shown for the free energy ($\Delta G = G_{\text{products}} - G_{\text{reactants}}$), enthalpy ($\Delta H = H_{\text{products}} - H_{\text{reactants}}$), and entropy ($T\Delta S = TS_{\text{products}} - TS_{\text{reactants}}$). The reference is taken as the value of the energy at 0 K. The entropic contribution of the hydrogen molecule $T(S_{H_2}(T) - S_{H_2}(T=0))$ is also shown separately.

Let us first consider route A with the polyaminoborane formation reaction (reaction 1). Energy differences between reactant A (BH_3NH_3) and products B ($BH_2NH_2 + H_2$) are shown in Fig. 7(a). The reaction free energy and enthalpy are negative for all temperatures in agreement with the experimentally observed exothermic character of this reaction. The experimental enthalpy value at 300 K (Ref. 8) is shown by the filled square and is comparable to the value found in our calculations. At lower temperatures the entropic contribution

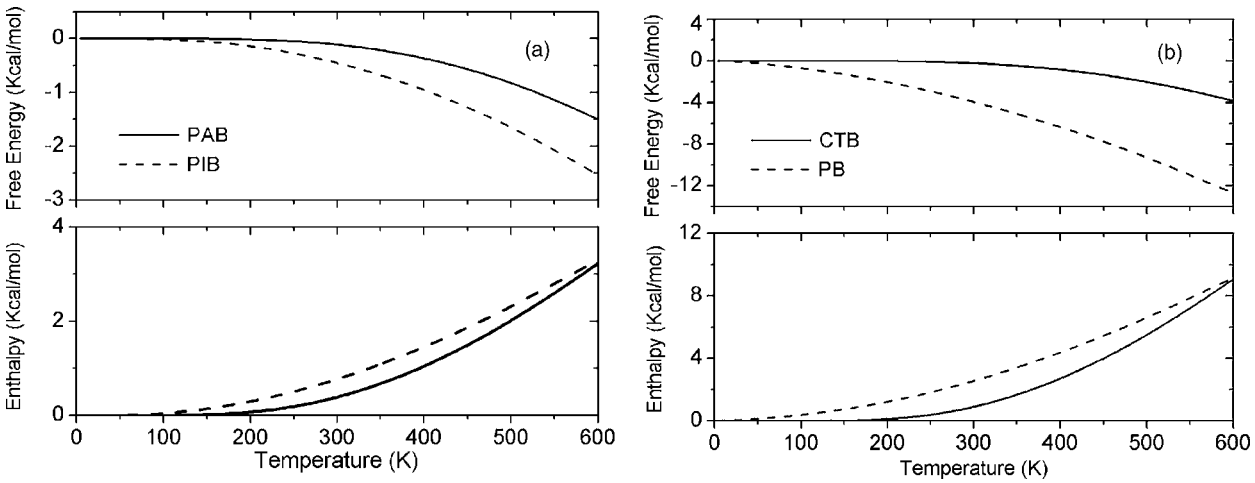

FIG. 6. Thermodynamic properties obtained by ab-initio calculations: free energy and enthalpy of ammonia-borane complexes as a function of temperature. The reference is the total electronic energy at 0 K (see Table III).

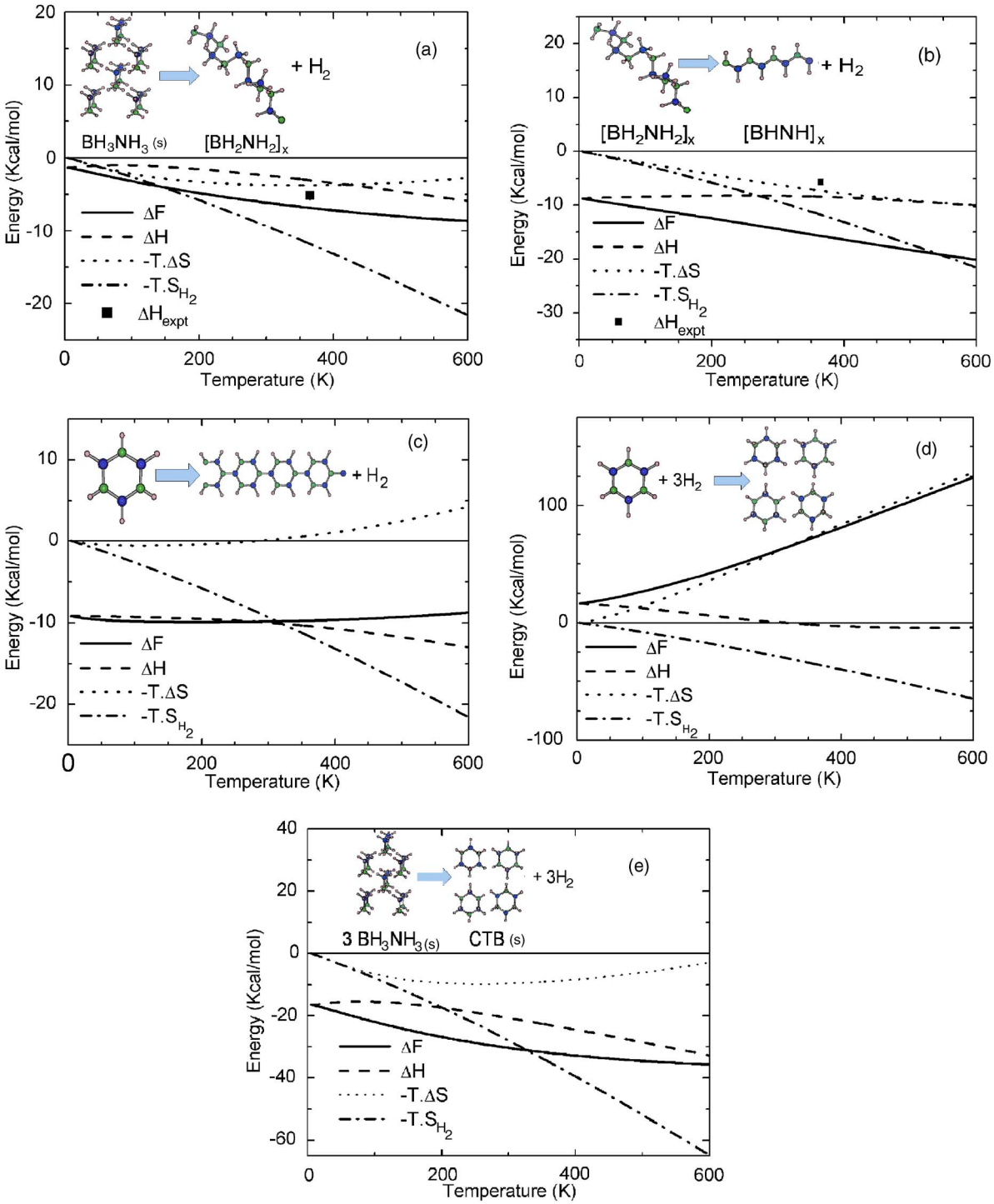

FIG. 7. (Color online) Thermodynamic properties for the thermal decomposition reactions of ammonia-borane complex reaction Helmholtz free energy difference (full line), reaction enthalpy (dashed line), reaction entropy (dotted), and the entropic term of the H_2 molecule (dotted-dashed line). The square represents the experimental data available for the reaction enthalpy (Refs. 8 and 9). (a) Polyaminoborane formation, (b) polyiminoborane formation, (c) borazine-cyclotriborazane cycle, (d) dehydropolymerization of borazine, and (e) ammonia borane into CTB transformation.

of the H_2 molecule dominates the reaction entropy. Above 300 K, the reaction entropy difference decreases with temperature as a result of the larger contribution of the ammonia-borane entropy. The polyiminoborane formation reaction (reaction 2), shown in Fig. 7(b), shows similar characteristics and is also exothermic. The free energy and enthalpy differences are even larger in this step (around −9.5 kcal/mol) than for the previous reaction.

We now turn our attention to the cyclic compound route as an alternate path for ammonia-borane decomposition. The possibility of dehydropolymerization of borazine following reaction 4 has been suggested.[38] We find a large negative reaction free energy and enthalpy difference varying between −8 and −12 kcal/mol with increase in temperature. It is interesting to note that the entropic contribution competition

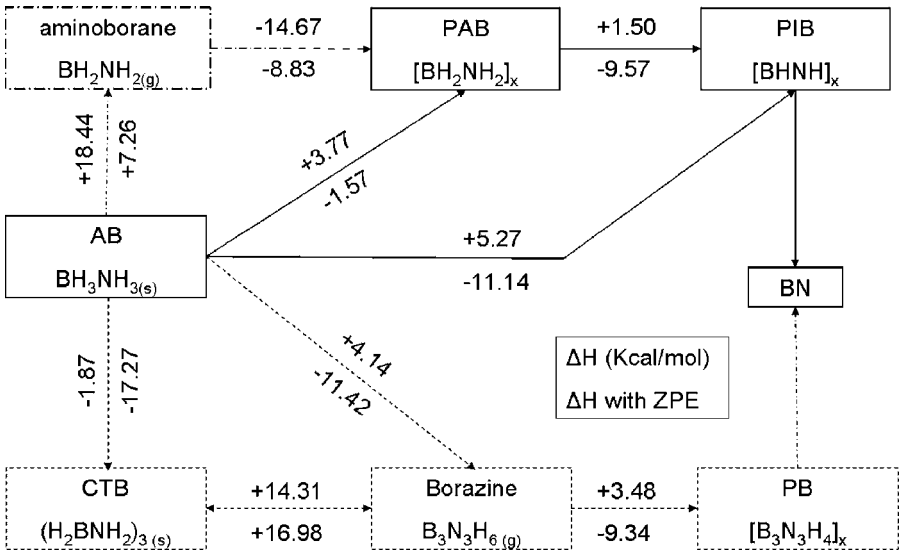

FIG. 8. Summary of the thermal decomposition of ammonia-borane compounds. The routes are the polymeric cycle (full line), the cyclic compounds (dashed line), and an alternative molecular path (dashed-dotted line). The enthalpies at 0 K without and with zero-point-energy correction are included.

between the borazine and hydrogen molecules leads to a nearly constant reaction free energy difference with temperature [see Fig. 7(c)].

Finally, we find that for the formation of cyclotriborazane by hydrogenation of borazine (reaction 5), the reaction free energy and enthalpy are positive at $T=0$ K, and respectively increase and decrease with temperature. At temperatures around 300 K the reaction becomes exothermic and the enthalpy remains nearly constant slightly below 0 kcal/mol [see Fig. 7(d)]. On the other hand, the transformation of ammonia borane to cyclotriborazane followed by hydrogen release is a strong exothermic reaction. The free energy and enthalpy reactions vary between −17 and −35 kcal/mol in the range of 0–600 K.

IV. DISCUSSION

By exploring the thermal decomposition of ammonia borane by first principles calculations, our results provide insights into the thermal stability of ammonia-borane complexes. From the theoretical point of view, it is clear from our results that DFT-GGA can capture the chemistry of these molecular systems. Computed bond lengths and vibrational frequencies agree well with experimental information. In particular, subtle bonding features, such as the shortening of the N–B bond in going from molecular ammonia borane to the solid state, are well represented in the GGA approximation. The dihydrogen bond between the hydrogen bonded to boron and the hydrogen bonded to nitrogen, responsible for the stability of AB in the solid state, is similarly described well. We find that the nitrogen-hydrogen bond has a covalent character while the hydrogen-boron bond is more ionic with the electrons polarized away from the boron nucleus. The computed vibrational properties of the ammonia-borane systems are in good agreement with published infrared measurements,[8,10,33,38] and variations in the H–B and H–N stretching modes correlate well to changes on the bond length.

Only for the ammonia-borane system can the calculated thermodynamic properties be validated by experimental data. Based on the quantitative agreement found for the vibrational properties, we believe that our calculations can also provide reliable thermodynamic data for the other systems. The enthalpy changes in the various decomposition reactions on the ammonia-borane systems are summarized in Fig. 8. We have shown the reaction enthalpies with and without zero-point energies to demonstrate the importance of this contribution. The zero-point energy (ZPE) changes the character of several reactions from endothermic (without the ZPE) to exothermic (with ZPE). Clearly, zero-point energy cannot be neglected when predicting reaction enthalpies in the ammonia-borane system.[11,16]

Our predictions for the heat release along the AB → PAB → PIB dehydrogenation path are in agreement with experimental studies[7,9,10] indicating that ammonia borane releases hydrogen along the polymeric route by two separate exothermic reactions. Using a low heating rate the two exothermic steps can be separated in experiments.[7,9] Polymeric aminoborane has been reported to be the main product in the first step of the ammonia-borane thermal decomposition, but molecular aminoborane and borazine have also been observed, and their amounts increase with increasing heating rate.[7,9] Our results indicate that the generation of borazine instead of PIB does not drastically change the reaction enthalpy for the full release of $2H_2$, though if borazine is produced during the conversion of AB to PAB, a larger exothermic heat would be found for the first H_2 release, than if only PAB were produced. This may explain why our predicted enthalpy for the reaction from AB to PAB is less negative than what has been found experimentally.[9] Another possibility for this discrepancy is that a more stable form of PIB exists than what we have used for our calculations. Limited experimental data indicates that this is an amorphous polymer,[7–9] while we have used a single infinite polymer chain in our calculation. It is possible, and likely, that interchain interactions in the amorphous solid lower the energy further from what we have calculated. In addition, there would be the effect of small oligomers saturated with BH_3 and NH_3 end groups which could lower energy as it has been recently obtained by Li *et al.*[15]

The results in Figs. 7 demonstrates that the reactions by

which ammonia borane decomposes all have negative free energy change indicating that the temperature at which hydrogen is released from these compounds is determined purely by the kinetics of the decomposition. This seems to be in agreement with the fact that different reaction temperatures are found for different heating rates[7,9] and may enable control of the reaction temperatures by using suitable catalysts. The exothermic nature of reactions does, however, confirm that regeneration will be difficult and may require very high hydrogen pressure.

When normalized to the release of one H_2 molecule, the reaction energies in Table III and Fig. 8 also give the chemical potential of hydrogen in the reactions. More specifically, the reaction energies are the negative of the chemical potential. Somewhat surprisingly, the chemical potential of hydrogen *increases* from reaction 1 (AB→PAB) to reaction 2 (PAB→PIB) suggesting that polymeric aminoborane is not a thermodynamically stable intermediate phase between ammonia-borane and polymeric iminoborane. This could be an artifact due to our approximation of the PAB state as a single infinite polymer chain, as discussed earlier, or could be real. In the latter case, it is still possible that PAB occurs as a metastable product along the kinetic decomposition path of AB to PIB. The fact that the nature and amount of decomposition products observed depend sensitively on the heating rate[7] seems to point at kinetically controlled product selection in the reactions rather than thermodynamic selection.

The dehydrocoupling borazine reaction (reaction 4—polyborazylene formation) has been successfully achieved in experiments when borazine is heated to 307 K.[33,37] Our data on Fig. 7(c) predict an exothermic reaction for the complete temperature range studied, indicating that for borazine, as for AB and PAB, the temperature at which hydrogen is released is kinetically controlled. The reverse hydrogenation of polyborazylene has been the focus of some recent studies.[33]

There have been experimental attempts to construct a reversible hydrogen storage system from the polymerization of borazine to cyclotriborazane. Borazine hydrogenation [reaction (5)] has been attempted by using Ni and Pd catalysts at temperatures in the ranges of 363–373 K (Ni) and 313–323 K (Pd).[40] Our calculated thermodynamic data [Fig. 7(d)] indicates that the hydrogenation of borazine is accompanied by a significant free energy increase for all temperatures which may explain the unsuccessful experimental attempts to produce cyclotriborazane. Instead, formation of a polymeric solid has been observed.[38] We have also explored the dehydrogenation reaction of the solid-solid transformation of ammonia borane into cyclotriborazane (reaction 6). Once more, our data predicts a strong exothermic character of reaction 6, and the kinetics would play a major role also in this reaction. The possible reversibility of the reaction should be achieved by using different chemical paths rather than a direct reversibility.

Our data as a whole support the findings that the rehydrogenation process of amino borane will be difficult. Both along the polymeric and cyclic ammonia-borane path are the dehydrogenation reactions exothermically leading to a strong positive free energy increase for the inverse hydrogenation reactions. Because of the positive reaction entropy in most hydrogen release reactions, an increase in temperature will only make the regeneration more difficult.

V. CONCLUSIONS

In summary, we have studied through first principles calculations the structural, electronic, vibrational, and thermodynamic properties of ammonia-borane complexes in the context of their potential application for hydrogen storage. We find that zero-point motion changes the enthalpy of many reactions from endothermic to exothermic when releasing hydrogen. From the prospect of hydrogen storage, it is unlikely that ammonia borane can be regenerated by using the ammonia-borane polymeric and borazine-cyclotriborazane cycles due to the strong exothermic character of the reactions. Alternative ways to modify the relative thermodynamic stability of hydrogenated and dehydrogenated compounds should be investigated for the practical use of ammonia borane as an on-board hydrogen storage material.

ACKNOWLEDGMENTS

This research was supported by the Department of Energy (DOE) Hydrogen Program, under Contract No. DE-FG02-05ER46253. Supercomputing resources from the San Diego Supercomputing Center are acknowledged.

[1] W. Grochola and P. O. Edwards, Chem. Rev. (Washington, D.C.) **104**, 1283 (2004).
[2] A. M. Seyad and D. M. Antonelli, Adv. Mater. (Weinheim, Ger.) **16**, 765 (2004).
[3] For a more general review, see www.hydrogen.energy.gov
[4] A. Gutowska, L. Li, Y. Shin *et al.*, Angew. Chem., Int. Ed. **44**, 3578 (2005).
[5] S. de Benedetto, M. Carewska, C. Cento, P. Gislon, M. Pasquali, S. Scaccia, and P. P. Prosisi, Thermochim. Acta **441**, 184 (2006).
[6] M. E. Bluhm, M. G. Bradley, R. Butterick III, U. Kusari, and L. G. Sneddon, J. Am. Chem. Soc. **128**, 7748 (2006).
[7] F. Baitalow, J. Baumann, G. Wolf, K. Jaenicke-Rößler, and G. Leitner, Thermochim. Acta **391**, 159 (2002).
[8] J. Baumann, F. Baitalow, and G. Wolf, Thermochim. Acta **430**, 9 (2005).
[9] G. Wolf, J. Baumann, F. Baitalow, and F. P. Hoffmann, Thermochim. Acta **343**, 19 (2000).
[10] G. Wolf, J. C. van Miltenburg, and U. Wolf, Thermochim. Acta **317**, 111 (1998).
[11] D. A. Dixon and M. Gutowski, J. Phys. Chem. A **109**, 5129 (2005).
[12] J. Zhang, S. Zhang, and Q. S. Li, J. Mol. Struct.: THEOCHEM **717**, 33 (2005).
[13] Q. S. Li, J. Zhang, and S. Zhang, Chem. Phys. Lett. **404**, 100 (2005).
[14] H. J. Himmel and H. Schnockel, Chem.-Eur. J. **8**, 2397 (2002).
[15] J. Li, S. M. Kathmann, G. K. Schenter, J. C. Linehan, T. Autrey, and M. Gutowski, Prepr. Pap. - Am. Chem. Soc., Div. Fuel Chem. **51**, 577 (2006).
[16] M. Gutowski and T. Autrey, Prepr. Pap. - Am. Chem. Soc., Div. Fuel Chem. **49**, 275 (2004).
[17] C. A. Morrison and M. M. Siddick, Angew. Chem., Int. Ed. **43**, 4780 (2004).
[18] W. Kohn and L. J. Sham, Phys. Rev. A **140**, 1133 (1965).
[19] G. Kresse and J. Furthmüller, Phys. Rev. B **54**, 11169 (1996).
[20] G. Kresse. and J. Furthmüller, Comput. Mater. Sci. **6**, 15 (1996).
[21] J. P. Perdew and Y. Wang, Phys. Rev. B **45**, 13244 (1992).
[22] J. P. Perdew, J. A. Chevary, S. H. Vosko, K. A. Jackson, M. R. Pederson, D. J. Singh, and C. Fiolhais, Phys. Rev. B **46**, 6671 (1992).
[23] P. E. Blöchl, Phys. Rev. B **50**, 17953 (1994).
[24] G. Kresse and D. Joubert, Phys. Rev. B **59**, 1758 (1999).
[25] W. T. Klooster, T. F. Koetzle, P. E. M. Siegbahn, T. B. Richardson, and R. H. Crabtree, J. Am. Chem. Soc. **121**, 6337 (1999).
[26] D. Jacquemin, E. A. Perpète, V. Wathelet, and J.-M. André, J. Phys.

Chem. A **108**, 9616 (2004).
[27] D. Jacquemin, J. Phys. Chem. A **108**, 9260 (2004).
[28] A. Abdurahman, M. Albrecht, A. Shukla, and M. Dolg, J. Chem. Phys. **110**, 8819 (1999).
[29] P. W. R. Corfield and S. G. Shore, J. Am. Chem. Soc. **95**, 1480 (1973).
[30] C. J. Cramer and W. L. Gladfelter, Inorg. Chem. **36**, 5358 (1997).
[31] K. W. Böddeker, S. G. Shore, and R. K. Bunting, J. Am. Chem. Soc. **88**, 4396 (1966).
[32] A. A. Maradudin, E. W. Montroll, G. H. Weiss, and I. P. Ipatova, *Theory of Lattice Dynamics in the Harmonic Approximation*, 2nd ed. (Academic, New York, 1971).
[33] D. G. Allis, M. E. Kosmowski, and B. S. Hudson, J. Am. Chem. Soc. **126**, 7756 (2004).
[34] A. D. Becke and K. E. Edgecombe, J. Chem. Phys. **92**, 5397 (1990).
[35] B. Silvi and A. Savin, Nature (London) **371**, 683 (1994).
[36] A. Savin, R. Nesper, S. Wengert, and T. F. Fässler, Angew. Chem., Int. Ed. Engl. **36**, 1808 (1997).
[37] P. Ravindran, P. Vajeeston, H. Fjellvåg, and A. Kjekshus, Comput. Mater. Sci. **30**, 349 (2004).
[38] N. Mohajeri and A. T. Raissi, report Florida Solar Energy Center, 2005, (unpublished); Mater. Res. Soc. Symp. Proc. **884E**, GG1.4.1 (2005).
[39] C. F. Hoon and E. C. Reynhardt, J. Phys. C **16**, 6129 (1983).
[40] E. Wiberg and A. Bolz, Ber. Dtsch. Chem. Ges. B **73**, 209 (1940).
[41] P. J. Fazen, E. E. Remsen, J. S. Beck, P. J. Carroll, A. R. McGhie, and L. G. Sneddon, Chem. Mater. **7**, 1942 (1995).